

Figure 5. Coordination polyhedra for the ten nearest molecular neighbors (a) in the orthorhombic structure, symmetry 222, and (b) in tetragonal protactinium metal, symmetry 4/*mmm*.

revealed that it exists in one of the forms of 1,2,3,4-tetra-bromocyclohexane<sup>11</sup> and in one polymorph of cyclotetra-methylenetetranitramine.<sup>12</sup>

The synthesis of  $U_4(\text{dmed})_8$  probably proceeds with a stepwise replacement of the diethylamide groups by dimethylethylenediamine. There is evidence from the color changes observed during the formation of  $U(\text{N}(\text{C}_2\text{H}_5)_2)_4$  for this type of stepwise addition.<sup>6</sup> Changing the reaction conditions might result in a greater yield of the tetramer. The U-U distance in the tetramer is slightly longer than in the trimer; so, as in the trimer molecule, it is unlikely that there will be any magnetic interactions above 4.2 K. A remarkable

characteristic of these uranium-amide systems is their tendency toward oligomerization. Further work on f-electron and d-electron metal amide complexes is necessary to determine the generality of this oligomerization reaction.

Registry No.  $U_4(\text{dmed})_8$ , 62743-74-2.

Supplementary Material Available: Data processing formulae and listing of structure factor amplitudes (6 pages). Ordering information is given on any current masthead page.

#### References and Notes

- (1) This work was done with support from the U.S. Energy Research and Development Administration.
- (2) J. G. Reynolds, A. Zalkin, D. H. Templeton, and N. M. Edelstein *Inorg. Chem.*, **16**, 599 (1977).
- (3) L. K. Templeton and D. H. Templeton, Abstracts, American Crystallographic Association Proceedings, Series 2, Vol. 1, 1973, p 143.
- (4) J. Waser, *Acta Crystallogr.*, **16**, 1091 (1963).
- (5) J. G. Reynolds, A. Zalkin, D. H. Templeton, and N. M. Edelstein, *Inorg. Chem.*, **15**, 2498 (1976).
- (6) J. G. Reynolds, A. Zalkin, D. H. Templeton, and N. M. Edelstein, *Inorg. Chem.*, **16**, 1090 (1977).
- (7) D. C. Bradley and M. H. Chisholm, *Acc. Chem. Res.*, **9**, 273 (1976), and references therein.
- (8) W. H. Zachariasen, *Acta Crystallogr.*, **5**, 19 (1952).
- (9) K. Volz, A. Zalkin, and D. H. Templeton, *Inorg. Chem.*, **15**, 1827 (1976).
- (10) L. K. Templeton, D. H. Templeton, N. Bartlett, and K. Seppelt, *Inorg. Chem.*, **15**, 2720 (1976).
- (11) E. W. Lund, *Acta Chem. Scand.*, **4**, 1109 (1950).
- (12) H. H. Cady, A. C. Larson, and D. T. Cromer, *Acta Crystallogr.*, **16**, 617 (1963).

Contribution from the Department of Chemistry, Texas A&M University, College Station, Texas 77843

## Local and Internuclear Carbonyl Scrambling in Pentacarbonyl-7*H*-indenediiron, $(\text{C}_9\text{H}_8)\text{Fe}_2(\text{CO})_5$ , and Tetracarbonyl-7*H*-indene(triethylphosphine)diiron, $(\text{C}_9\text{H}_8)\text{Fe}_2(\text{CO})_4(\text{PEt}_3)$

F. ALBERT COTTON\* and BRIAN E. HANSON

Received December 29, 1976

AIC60932L

The molecule  $(\text{C}_9\text{H}_8)\text{Fe}_2(\text{CO})_5$  is observed to undergo two fluxional processes. Localized scrambling in the  $\text{Fe}(\text{CO})_3$  moiety has a coalescence temperature of  $-134^\circ\text{C}$ , one of the lowest known for such a process. On the other hand, internuclear carbonyl scrambling occurs with a higher activation energy than in other similar molecules. Coalescence is observed at ca.  $120^\circ\text{C}$ , and the activation parameters for internuclear scrambling have been estimated to be  $E_a = 17.7$  (3) kcal mol<sup>-1</sup> and  $\log A = 12.3$ . Crystals of  $(\text{C}_9\text{H}_8)\text{Fe}_2(\text{CO})_5$  belong to the orthorhombic system, space group *Pbca*. Unit cell parameters are  $a = 14.968$  (5),  $b = 13.576$  (5), and  $c = 13.124$  (7) Å. The Fe-Fe bond length is 2.782 (1) Å. In the triethylphosphine derivative,  $(\text{C}_9\text{H}_8)\text{Fe}_2(\text{CO})_4\text{PEt}_3$ , selective internuclear scrambling involving three of the four carbonyl ligands is observed, in close analogy to our earlier observations on (guaiazulene) $\text{Fe}_2(\text{CO})_4\text{PEt}_3$ .

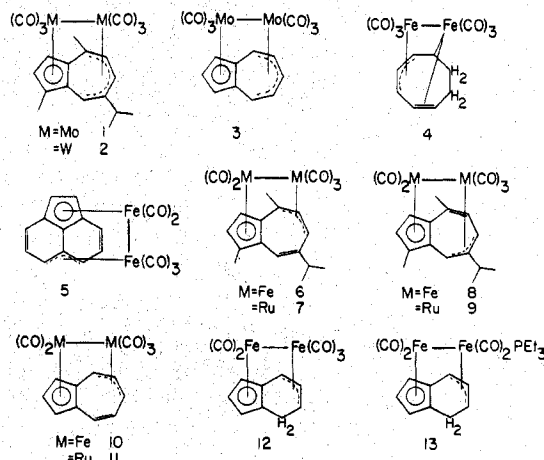
### Introduction

In a recent paper<sup>1</sup> we have discussed conditions governing internuclear carbonyl scrambling in binuclear compounds having an  $(\text{OC})_n\text{M}-\text{M}'(\text{CO})_m$  moiety bonded to a polyene or polyenyl group. On the basis of facts known at the present time, the following rules may be suggested.

(1)  $n$  should not be equal to  $m$ . Thus, for  $(\text{C}_{15}\text{H}_{18})\text{Mo}_2(\text{CO})_6$  (1),<sup>2</sup>  $(\text{C}_{15}\text{H}_{18})\text{W}_2(\text{CO})_6$  (2),<sup>3</sup>  $(\text{C}_8\text{H}_{10})\text{Fe}_2(\text{CO})_6$  (4),<sup>4</sup> and  $(\text{C}_{10}\text{H}_{12})\text{Fe}_2(\text{CO})_6$ ,<sup>5</sup> a bicyclic homologue of 4, in all of which  $n = m = 3$ , only localized scrambling is observed.

(2) The  $\pi$ -electron density of the polyene ligand must be capable of a redistribution to allow for the transfer of a carbonyl ligand from one metal atom to the other. Thus no internuclear scrambling is observed in  $(\text{C}_{12}\text{H}_8)\text{Fe}_2(\text{CO})_5$ ,<sup>6</sup> 5, at  $75^\circ\text{C}$ .

The molecules that have been observed, 6-11, to undergo internuclear exchange in this class of compounds have guaiazulene<sup>1</sup> or azulene<sup>6</sup> as the polyene ligand, with  $n = 2$  and  $m = 3$ . In the iron derivatives of azulene and guaiazulene internuclear exchange is sufficiently facile that it is observed at room temperature.



Another molecule in this class of compounds, i.e., one that meets our empirical requirements for internuclear scrambling, is (7*H*-indene) $\text{Fe}_2(\text{CO})_5$  (12). A recent carbon-13 NMR study<sup>8</sup> of this compound failed to show internuclear scrambling

up to 30 °C. This made an interesting contrast with our observation that **6**, **8**, and **10** exhibit this type of fluxionality at room temperature. Also, the  $\text{Fe}(\text{CO})_3$  moiety was observed to be scrambling rapidly at -50 °C. To us, these fragmentary data suggested that a complete investigation of the stereodynamic behavior of **12** would be worthwhile, and such a study, including an x-ray crystallographic confirmation of the presumed structure, has been completed. The variable-temperature carbon-13 NMR spectrum has been studied from -140 to +120 °C. Carbon-13 NMR studies on  $(7H\text{-indene})\text{Fe}_2(\text{CO})_4\text{PEt}_3$  have yielded additional information on the scrambling processes. Our results show that our previous discussion of internuclear scrambling is valid also for **12** and **13**.

### Experimental Section

**Preparation of  $(\text{C}_9\text{H}_8)\text{Fe}_2(\text{CO})_5$ .** Indene, technical grade, was distilled at reduced pressure and stored under nitrogen. Diiron nonacarbonyl (3.0 g, 8.3 mmol) was suspended in 75 mL of hexane; indene (1 mL, 8.6 mmol) was syringed into the slurry. The mixture was stirred at room temperature for 20 h under an atmosphere of nitrogen. After removal of solvent the residue was extracted with 1:1 hexane- $\text{CH}_2\text{Cl}_2$  and placed on a chromatography column, 30 × 2.5 cm, packed with Florisil, 100-200 mesh. Elution with 1:1 hexane- $\text{CH}_2\text{Cl}_2$  brought triiron dodecacarbonyl down the column first, followed by an orange band containing  $(\text{C}_9\text{H}_8)\text{Fe}_2(\text{CO})_5$ . A brown band could also be eluted by increasing the ratio of  $\text{CH}_2\text{Cl}_2$ . The brown material, which showed a bridging carbonyl band in the infrared spectrum, was not investigated further.  $(\text{C}_9\text{H}_8)\text{Fe}_2(\text{CO})_5$  has absorptions in the carbonyl region at 2038, 1983, and 1971  $\text{cm}^{-1}$ . Anal. Calcd for  $\text{C}_{14}\text{H}_{18}\text{O}_5\text{Fe}_2$ : C, 45.71; H, 2.19. Found: C, 46.02; H, 2.27. The mass spectrum shows a peak with  $m/e$  368 (calcd for  $\text{C}_{14}\text{H}_{18}\text{O}_5\text{Fe}_2^+$   $m/e$  368).  $(\text{C}_9\text{H}_8)\text{Fe}_2(\text{CO})_5$  was enriched to approximately 10% in  $^{13}\text{C}$  by irradiating the compound in  $\text{CH}_2\text{Cl}_2$  with a Norelco 250-W lamp under an atmosphere of carbon monoxide enriched to 90% in  $^{13}\text{C}$ .

**Preparation of  $(\text{C}_9\text{H}_8)\text{Fe}_2(\text{CO})_4\text{PEt}_3$ .** Enriched  $(\text{C}_9\text{H}_8)\text{Fe}_2(\text{CO})_5$  (0.5 g, 1.36 mmol) was dissolved in 30 mL of benzene in a Pyrex flask, and triethylphosphine (0.6 mL, 4.2 mmol) was syringed into the solution. The solution was then irradiated for 20 h with a Norelco 250 high-pressure mercury lamp. Removal of the solvent left an orange-brown oil which was taken up in a minimum of hexane-benzene and chromatographed on Florisil, eluting first with 2:1 hexane-benzene and slowly increasing the ratio of benzene as needed to elute the various bands. The first band eluted corresponded to starting material,  $(\text{C}_9\text{H}_8)\text{Fe}_2(\text{CO})_5$ . The major component of the reaction was then eluted as a red-orange band, with carbonyl stretching frequencies (in hexane) at 1955 (s) and 1943 (s)  $\text{cm}^{-1}$ . The mass spectrum showed  $\text{M}^+$  at  $m/e$  458. The carbon-13 NMR spectrum is wholly consistent with substitution of one CO by  $\text{PEt}_3$ . This substitution occurs on the iron atom bonded to the allylic portion of 7H-indene.

**Carbon-13 NMR Measurements.** These were made on a JEOL PS100/Nicolet 1080 Fourier transform spectrometer operating at 25.036 MHz. A tilt angle of 40° and repetition rate of 1.2 s were employed to collect from 3000 to 5000 scans per spectrum for **12** and from 10000 to 15000 scans per spectrum for **13**.

NMR solvents for **12** were as follows: from -140 to -117 °C, 15%  $\text{CD}_2\text{Cl}_2$ , 80%  $\text{CHFCl}_2$ , and 5%  $\text{CS}_2$ ; from -107 to -42 °C, 10% acetone- $d_6$ , 85%  $\text{CHFCl}_3$ , and 5%  $\text{CS}_2$ ; from 24 to 64 °C, 25%  $\text{C}_2\text{D}_2\text{Cl}_4$ , 70%  $\text{C}_2\text{H}_2\text{Cl}_4$ , and 5%  $\text{CS}_2$ . The high-temperature spectra shown in Figure 2 and the spectra for **13** shown in Figure 4 were obtained in 10% toluene- $d_8$ , 85% toluene, and 5% TMS. Chemical shifts were measured from  $\text{CS}_2$  or TMS ( $\delta_{\text{CS}_2} = \delta_{\text{TMS}} - 192.8$ ). Approximately 5 mg of  $\text{C}_6\text{H}_5\text{I}(\text{acac})_3$  was added to each sample.

Computer simulations of the high-temperature spectra of **12** were performed using a random-exchange matrix as described previously.<sup>7</sup>

**Crystal Data and Structure Determination.** A crystal of dimensions 0.3 × 0.3 × 0.4 mm was grown from toluene at -20 °C. The crystal was sealed under argon in a glass capillary. A Syntex P1 diffractometer was used for preliminary x-ray examination and data collection. The crystal was found to be orthorhombic belonging to the space group  $Pbca$ .  $\omega$  scans of several reflections had peak widths less than 0.20° at half-height. Cell constants were obtained by centering on 15 reflections in the range  $20 < 2\theta < 30^\circ$ ;  $a = 14.968$  (5) Å,  $b = 13.576$  (5) Å,  $c = 13.124$  (7) Å, and  $V = 2666.7$  (1.9) Å<sup>3</sup>.

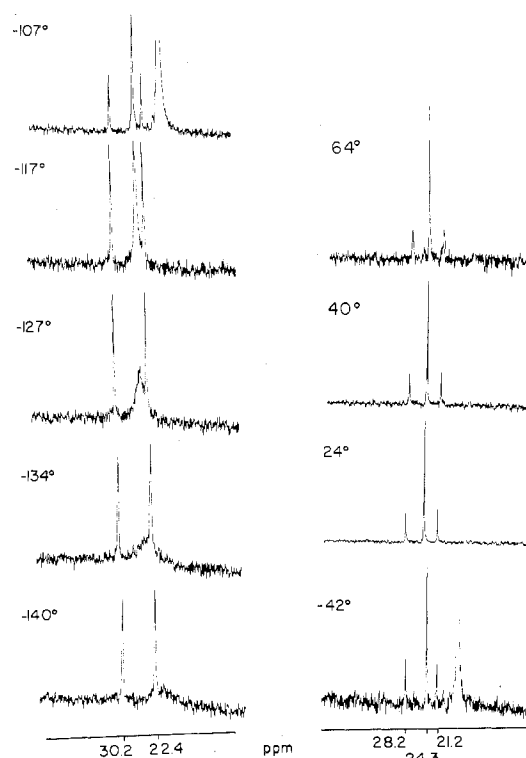


**Figure 1.** Carbon-13 NMR spectra for  $(7H\text{-indene})\text{Fe}_2(\text{CO})_5$  at various temperatures. Chemical shifts are measured downfield from  $\text{CS}_2$  ( $\delta_{\text{CS}_2} = \delta_{\text{TMS}} - 192.8$ ).

Intensities were measured at  $22 + 4$  °C using the  $\theta$ - $2\theta$  scan technique. Mo  $K\alpha$  radiation was used to collect 2731 reflections in the range  $0 < 2\theta < 50^\circ$ . Of these, 1535 reflections of  $I > 3\sigma(I)$  were used as observed data. The linear absorption coefficient is  $22.5 \text{ cm}^{-1}$ ; absorption corrections were omitted.

Software provided by Enraf-Nonius was used to solve and refine the structure on a PDP 11/45 computer.<sup>9</sup> The two iron atoms were located from an  $E$  map generated using the starting phase set with the highest figure of merit from the program MULTAN based on 264 reflections with  $E$  values greater than 1.6. A difference Fourier map following three cycles of least-squares refinement on the iron positions revealed the five carbonyl ligands. Another difference Fourier map following three least-squares cycles on 12 atoms revealed the indene ring. Full-matrix least-squares refinement with anisotropic temperature factors for all nonhydrogen atoms converged in three cycles to give final discrepancy indices of  $R_1 = 0.046$  and  $R_2 = 0.060$  and an error in an observation of unit weight of 1.295. A table of calculated and observed structure factor amplitudes is available.<sup>10</sup>

### Results

**Carbon-13 NMR Spectra.** The variable-temperature NMR spectra for **12** are shown in Figure 1 from -140 to +64 °C. Decomposition occurred in the solvents tetrachloroethane and  $\text{CS}_2$  thus preventing measurement of the spectrum above 64 °C in this solvent mixture. The use of toluene as solvent allowed us to obtain spectra as high as 120 °C; these spectra are shown in Figure 2. Coalescence for internuclear scrambling occurs at ca. 120 °C. The high-temperature spectra were satisfactorily simulated using a random-exchange matrix.  $E_a$ , the Arrhenius activation energy for internuclear exchange, was found to be 17.7 (3) kcal mol<sup>-1</sup>, coupled with a log  $A$  value of 12.3.

Local carbonyl scrambling in the  $\text{Fe}(\text{CO})_3$  fragment is a very facile process. Coalescence occurs at ca. -134 °C.

The NMR spectra at various temperatures for **13** are shown in Figure 3. Triethylphosphine substitution increased the activation barrier for internuclear scrambling. Thus, spectra extending to the coalescence range could not be obtained for

Table I. Positional and Thermal Parameters and Their Estimated Standard Deviations

Atom	<i>x</i>	<i>y</i>	<i>z</i>	<i>B</i> <sub>11</sub>	<i>B</i> <sub>22</sub>	<i>B</i> <sub>33</sub>	<i>B</i> <sub>12</sub>	<i>B</i> <sub>13</sub>	<i>B</i> <sub>23</sub>
Fe(1)	0.38933 (6)	0.44847 (6)	0.21748 (6)	0.00331 (3)	0.00395 (4)	0.00427 (4)	0.00008 (8)	0.00014 (7)	0.00020 (8)
Fe(2)	0.28603 (6)	0.30003 (7)	0.30394 (6)	0.00328 (4)	0.00462 (5)	0.00447 (4)	-0.00087 (8)	0.00012 (8)	-0.00034 (9)
O(1)	0.4891 (3)	0.2825 (3)	0.1350 (4)	0.0058 (3)	0.0064 (3)	0.0086 (4)	0.0031 (5)	0.0027 (5)	-0.0017 (6)
O(2)	0.2263 (3)	0.4591 (4)	0.0939 (4)	0.0053 (3)	0.0137 (5)	0.0075 (3)	-0.0007 (6)	-0.0040 (5)	0.0071 (7)
O(3)	0.4774 (4)	0.5838 (4)	0.0774 (4)	0.0091 (3)	0.0071 (3)	0.0086 (4)	-0.0038 (6)	0.0066 (6)	0.0029 (6)
O(4)	0.3803 (4)	0.1223 (4)	0.2433 (6)	0.0059 (3)	0.0061 (3)	0.0175 (6)	0.0029 (5)	0.0029 (8)	-0.0028 (8)
O(5)	0.1398 (3)	0.2549 (5)	0.1669 (4)	0.0051 (3)	0.0119 (4)	0.0083 (3)	-0.0016 (6)	-0.0035 (5)	-0.0059 (7)
C(1)	0.4466 (4)	0.3433 (5)	0.1686 (5)	0.0037 (3)	0.0052 (4)	0.0054 (4)	0.0009 (6)	-0.0005 (6)	-0.0008 (7)
C(2)	0.2892 (5)	0.4526 (5)	0.1444 (5)	0.0043 (3)	0.0073 (4)	0.0045 (3)	-0.0001 (7)	0.0005 (6)	0.0022 (7)
C(3)	0.4439 (5)	0.5331 (5)	0.1343 (5)	0.0050 (3)	0.0046 (4)	0.0065 (4)	0.0005 (6)	0.0024 (7)	-0.0003 (7)
C(4)	0.3452 (4)	0.1959 (5)	0.2658 (6)	0.0033 (3)	0.0060 (4)	0.0088 (5)	-0.0026 (6)	-0.0006 (7)	0.0012 (8)
C(5)	0.2000 (5)	0.2743 (5)	0.2177 (5)	0.0046 (3)	0.0056 (4)	0.0049 (4)	0.0008 (6)	0.0008 (6)	-0.0016 (6)
C(6)	0.2101 (5)	0.3983 (5)	0.3937 (5)	0.0050 (3)	0.0075 (5)	0.0049 (4)	-0.0008 (7)	0.0024 (6)	-0.0032 (7)
C(7)	0.2134 (5)	0.3025 (5)	0.4399 (5)	0.0052 (3)	0.0093 (5)	0.0048 (4)	-0.0019 (8)	0.0018 (7)	-0.0005 (8)
C(8)	0.3031 (5)	0.2768 (6)	0.4606 (5)	0.0053 (4)	0.0090 (5)	0.0044 (4)	-0.0041 (7)	0.0001 (6)	0.0026 (8)
C(9)	0.4576 (4)	0.3678 (5)	0.4218 (5)	0.0035 (3)	0.0076 (5)	0.0056 (4)	-0.0026 (6)	-0.0031 (6)	0.0026 (7)
C(10)	0.4797 (4)	0.4493 (5)	0.3471 (5)	0.0045 (3)	0.0053 (4)	0.0049 (4)	-0.0020 (6)	-0.0019 (6)	-0.0012 (7)
C(11)	0.4272 (5)	0.5362 (5)	0.3377 (5)	0.0049 (3)	0.0058 (4)	0.0053 (4)	-0.0015 (6)	-0.0001 (6)	-0.0036 (7)
C(12)	0.3333 (5)	0.5242 (5)	0.3455 (5)	0.0052 (3)	0.0053 (4)	0.0047 (3)	-0.0002 (6)	0.0008 (6)	-0.0031 (6)
C(13)	0.2994 (4)	0.4313 (4)	0.3874 (4)	0.0035 (3)	0.0055 (4)	0.0041 (3)	-0.0004 (6)	0.0003 (5)	-0.0018 (6)
C(14)	0.3580 (4)	0.3563 (5)	0.4257 (4)	0.0049 (3)	0.0060 (4)	0.0039 (3)	-0.0025 (6)	-0.0012 (6)	0.0002 (7)

<sup>a</sup> The form of the anisotropic thermal parameter is  $\exp[-(B_{11}h^2 + B_{22}k^2 + B_{33}l^2 + B_{12}hk + B_{13}hl + B_{23}kl)]$ .

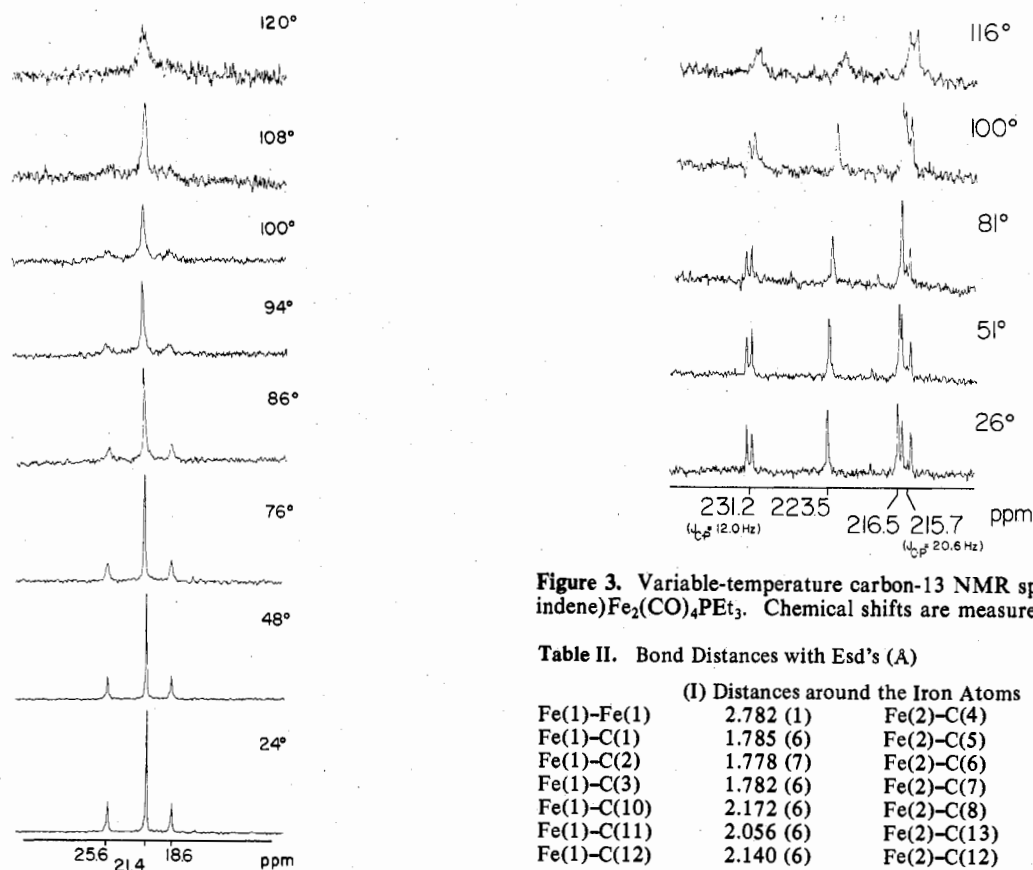


Figure 2. High-temperature spectra for (7*H*-indene) $\text{Fe}_2(\text{CO})_5$  recorded in toluene. Chemical shifts are measured from  $\text{CS}_2$ .

this compound because extensive decomposition occurs above 116 °C. It can be seen that the doublet centered at 215.7 ppm with  $J_{\text{C-P}} = 20.6$  Hz remains sharp even at 116 °C while each of the other three signals has broadened appreciably, the other doublet (at 231.2 ppm) having lost the coupling to  $^{31}\text{P}$ . It is to be noted that the relative chemical shifts of the signals at 216.5 and 215.7 ppm at 26 °C change slightly with temperature, so that at 116 °C the broadened singlet lies right under the doublet.

**Crystal Structure of (7*H*- $\text{C}_9\text{H}_8$ ) $\text{Fe}_2(\text{CO})_5$ .** The positional

Figure 3. Variable-temperature carbon-13 NMR spectra of (7*H*-indene) $\text{Fe}_2(\text{CO})_4\text{PEt}_3$ . Chemical shifts are measured from TMS.

Table II. Bond Distances with Esd's (Å)

(I) Distances around the Iron Atoms			
Fe(1)-Fe(1)	2.782 (1)	Fe(2)-C(4)	1.742 (8)
Fe(1)-C(1)	1.785 (6)	Fe(2)-C(5)	1.747 (7)
Fe(1)-C(2)	1.778 (7)	Fe(2)-C(6)	2.111 (6)
Fe(1)-C(3)	1.782 (6)	Fe(2)-C(7)	2.087 (6)
Fe(1)-C(10)	2.172 (6)	Fe(2)-C(8)	2.094 (6)
Fe(1)-C(11)	2.056 (6)	Fe(2)-C(13)	2.103 (5)
Fe(1)-C(12)	2.140 (6)	Fe(2)-C(12)	2.072 (6)
(II) Carbon-Oxygen Distances			
C(1)-O(1)	1.132 (7)	C(4)-O(1)	1.167 (8)
C(2)-O(2)	1.153 (7)	C(5)-O(6)	1.150 (7)
C(3)-O(3)	1.134 (7)		
(III) Bonds within the Indene Ligand			
C(6)-C(7)	1.436 (10)	C(10)-C(11)	1.424 (9)
C(7)-C(8)	1.411 (10)	C(11)-C(12)	1.424 (9)
C(8)-C(14)	1.431 (8)	C(12)-C(13)	1.466 (8)
C(9)-C(10)	1.515 (8)	C(13)-C(6)	1.410 (8)
C(9)-C(14)	1.497 (8)	C(13)-C(14)	1.436 (8)

and thermal parameters are listed in Table I, and the bond lengths and bond angles are presented in Tables II and III, respectively. A drawing of the molecular structure appears

Table III. Bond Angles with Esd's (deg)

(I) Angles around the Iron Atoms	
Fe(2)-Fe(1)-C(1)	80.29 (20)
C(2)	77.04 (20)
C(3)	166.21 (21)
C(1)-Fe(1)-C(2)	103.56 (29)
C(3)	94.46 (27)
C(2)-Fe(1)-C(3)	89.28 (25)
Fe(1)-Fe(2)-C(4)	100.98 (21)
C(5)	106.84 (21)
C(4)-Fe(2)-C(5)	91.39 (30)
(II) Angles within the Carbonyl Ligands	
Fe(1)-C(1)-O(1)	173.54 (56)
Fe(1)-C(2)-O(2)	176.37 (57)
Fe(1)-C(3)-O(3)	176.47 (59)
Fe(2)-C(4)-O(4)	175.37 (59)
Fe(2)-C(5)-O(5)	175.02 (58)
(III) Angles within the Indene Ligand	
C(13)-C(6)-C(7)	106.27 (0.59)
C(6)-C(7)-C(8)	109.82 (0.61)
C(7)-C(8)-C(14)	107.20 (62)
C(8)-C(14)-C(13)	107.37 (55)
C(6)-C(13)-C(14)	109.27 (54)
C(6)-C(13)-C(12)	128.52 (57)
C(8)-C(14)-C(9)	131.29 (60)
C(14)-C(9)-C(10)	108.43 (49)
C(9)-C(10)-C(11)	122.84 (0.55)
C(10)-C(11)-C(12)	116.38 (55)
C(11)-C(12)-C(13)	117.92 (55)
C(12)-C(13)-C(14)	122.16 (51)
C(13)-C(14)-C(9)	121.30 (52)

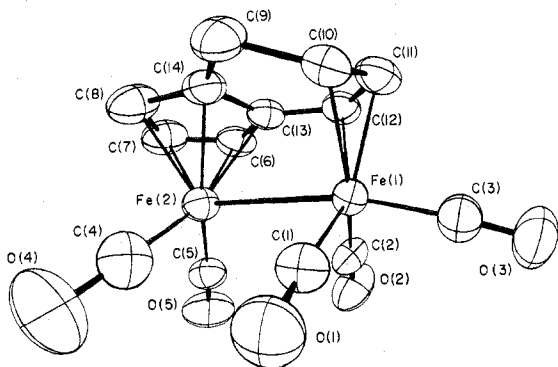


Figure 4. A view of the molecule  $(7H\text{-indene})\text{Fe}_2(\text{CO})_5$ . Atoms are drawn to enclose 50% of the electron density, and the atom-numbering scheme employed in Tables I-III is defined.

as Figure 4; the atomic numbering scheme used in the tables is defined there.

There are two important observations to be made from the crystallographic data on **12**. First, the Fe-Fe bond length is quite long, 2.782 (1) Å. A long Fe-Fe bond is characteristic for this type of molecule; (guaiazulene) $\text{Fe}_2(\text{CO})_5$  (**8**), (azulene) $\text{Fe}_2(\text{CO})_5$  (**10**), and (acenaphthalene) $\text{Fe}_2(\text{CO})_5$  (**5**) have Fe-Fe bond lengths of 2.80,<sup>1</sup> 2.78,<sup>11</sup> and 2.77 Å,<sup>12</sup> respectively. Second, the six-membered ring of 7H-indene is distorted away from planarity due to the methylene carbon atom (C<sub>9</sub> in our numbering scheme). The other five atoms in the ring, C(10)-C(14), are roughly coplanar.

### Discussion

The general purpose of this investigation has been fulfilled. The compounds **12** and **13** have been shown to have stereodynamic behavior qualitatively analogous to that of their azulene and guaiazulene analogues **6-11**. There are, however, very sizable quantitative differences. First, the local scrambling in the  $\text{Fe}(\text{CO})_3$  group is very much more facile in this case than in the azulene analogues. This is, in fact, the least hindered  $\text{Fe}(\text{CO})_3$  scrambling process so far reported for any  $\text{Fe}(\text{CO})_3$  group whose other attachments are to another

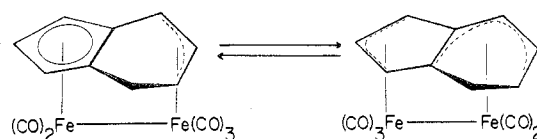


Figure 5. Proposed intermediate for internuclear scrambling in  $(7H\text{-indene})\text{Fe}_2(\text{CO})_5$ .

metal atom and to an  $\eta^3$ -allyl moiety. On the other hand, internuclear CO scrambling in this case requires higher thermal activation energy than in the azulene analogues.

Activation energies for  $\text{Fe}(\text{CO})_3$  scrambling vary considerably over the range of compounds studied, roughly from 7 to 15 kcal/mol,<sup>7</sup> and the factors influencing the ease of such scrambling are not well understood. For the  $\text{Fe}(\text{CO})_3$  group in **12** the activation energy can be estimated at about 6 kcal/mol from the approximate coalescence temperature of  $-134^\circ\text{C}$  and assuming that the separation of lines in the slow-exchange limit would be comparable to that observed<sup>7</sup> in compound **10**.

The higher activation energy for internuclear scrambling in **12** as compared to the same type process in the azulene and guaiazulene analogues, **6**, **8**, and **10**, can be understood in terms of the mechanism we have proposed<sup>1</sup> in these earlier studies. This mechanism as applied to **12** is shown in Figure 5.

The postulated intermediate is formed by transfer of one carbonyl group from the  $\text{Fe}(\text{CO})_3$  moiety to the  $\text{Fe}(\text{CO})_2$  group with concomitant redistribution of the  $\pi$ -electron density of the indene to form a new allyl group in the five-membered ring and a pentadienyl group in the six-membered ring. For the pentadienyl portion to be an effective ligand it should be nearly planar. Crystallographically, the five atoms forming the pentadienyl moiety are not coplanar. The analogous five atoms in (guaiazulene) $\text{Fe}_2(\text{CO})_5$ , **6**, are also nonplanar, but the energy requirements for achieving planarity of five atoms in the postulated intermediate should be greater in a six-membered ring with one  $\text{sp}^3$ -hybridized carbon than in a seven-membered ring where all carbon atoms are  $\text{sp}^2$  hybridized. The long Fe-Fe bond length can be ruled out as a reason for the high activation energy in **12** since **5**, **6**, **8**, **10**, (guaiazulene) $\text{Fe}_2(\text{CO})_4\text{PET}_3$ , and **12** all have similar Fe-Fe band lengths of approximately 2.8 Å.

**Significance of Internuclear Scrambling in 13.** Internuclear scrambling in **13** occurs in the same unique manner as observed for (guaiazulene) $\text{Fe}_2(\text{CO})_4\text{PET}_3$ . The two carbonyl groups on the  $\text{Fe}(\text{CO})_2$  fragment and only one of the carbonyl groups on the  $\text{Fe}(\text{CO})_2\text{PET}_3$  fragment are seen to exchange. As before, only one carbonyl may pass from the  $\text{Fe}(\text{CO})_2\text{PET}_3$  fragment to the  $\text{Fe}(\text{CO})_2$  fragment, but it is not possible to determine which CO participates in the exchange with the data at hand.

**Acknowledgment.** We thank the Robert A. Welch Foundation for support under Grant No. A494. We also thank Drs. B. A. Frenz and J. M. Troup of the Molecular Structure Corp. for assistance.

**Supplementary Material Available:** Listing of structure factors for compound **12** (7 pages). Ordering information is given on any current masthead page.

**Registry No.**  $(\text{C}_9\text{H}_8)\text{Fe}_2(\text{CO})_5$ , 59714-91-9;  $(\text{C}_9\text{H}_8)\text{Fe}_2(\text{CO})_4\text{PET}_3$ , 62707-84-0; diiron nonacarbonyl, 15321-51-4; <sup>13</sup>C, 14762-74-4.

### References and Notes

- F. A. Cotton, B. E. Hanson, J. R. Kolb, P. Lahuerta, G. G. Stanley, B. R. Stults, and A. J. White, *J. Am. Chem. Soc.*, **99**, 3673 (1977).
- (a) F. A. Cotton, D. L. Hunter, and P. Lahuerta, *J. Organomet. Chem.*, **87**, C42 (1975); (b) F. A. Cotton, P. Lahuerta, and B. R. Stults, *Inorg. Chem.*, **15**, 1866 (1976).
- F. A. Cotton and B. E. Hanson, *Inorg. Chem.*, **15**, 2806 (1976).
- F. A. Cotton, D. L. Hunter, and P. Lahuerta, *J. Am. Chem. Soc.*, **97**, 1046 (1975).
- F. A. Cotton and D. L. Hunter, *J. Am. Chem. Soc.*, **97** 5739 (1975).

- (6) F. A. Cotton, D. L. Hunter, and P. Lahuerta, *Inorg. Chem.*, **14**, 511 (1975).  
 (7) F. A. Cotton, B. E. Hanson, J. R. Kolb, and P. Lahuerta, *Inorg. Chem.*, **16**, 89 (1977).  
 (8) D. G. Lippard, H. J. Hansen, K. Bachmann, and W. V. Phillipsborn, *J. Organomet. Chem.*, **110**, 359 (1976).

- (9) Computations were performed at the Molecular Structure Corp., College Station, Tex. 77840.  
 (10) Supplementary Material.  
 (11) M. R. Churchill, *Inorg. Chem.*, **6**, 190 (1967).  
 (12) M. R. Churchill and J. Wormald, *Chem. Commun.*, 1597 (1968).

Contribution from the Department of Chemistry, Texas A&M University, College Station, Texas 77843

## Structure of the High-Temperature Form of Osmium(IV) Chloride

F. ALBERT COTTON\* and CATHERINE E. RICE

Received January 13, 1977

AIC70020Z

The high-temperature polymorph of OsCl<sub>4</sub> has been prepared in crystalline form by direct reaction of the elements; its structure has been determined by x-ray diffraction techniques. The space group is *Cmmm*. Unit cell dimensions are as follows:  $a = 7.929$  (2),  $b = 8.326$  (2),  $c = 3.560$  (1) Å;  $V = 235.0$  (1) Å<sup>3</sup>;  $Z = 2$ ;  $d = 4.69$  g cm<sup>-3</sup>. The structure, which consists of infinite chains of OsCl<sub>6</sub> octahedra sharing opposite edges with uniform Os–Os separations along the chains, appears to be the first AB<sub>4</sub> structure of its type. The Os–Os separation along the chain is 3.560 (1) Å, the Os–Cl(br) distance is 2.378 (2) Å, and the Os–Cl(nonbr) distance is 2.261 (4) Å. The structural and metal–metal bonding trends in nonmolecular transition metal tetrachlorides are discussed.

### Introduction

The highest known chloride of osmium is the tetrachloride, first prepared early in this century.<sup>1</sup> Two polymorphs have been reported: an orthorhombic high-temperature form, made by reaction of osmium metal with chlorine,<sup>1–3</sup> SO<sub>2</sub>Cl<sub>2</sub>,<sup>4</sup> or CCl<sub>4</sub>,<sup>5</sup> at 400–600 °C, and a cubic low-temperature form, made by reacting OsO<sub>4</sub> with SOCl<sub>2</sub> at reflux<sup>5</sup> or at room temperature.<sup>6</sup> In both cases only powder diffraction data were recorded. Magnetic susceptibilities<sup>5–7</sup> have also been reported for both forms of OsCl<sub>4</sub>, but no detailed structural information has been available, making this the only existing transition metal tetrachloride of unknown structure.

In the tetrachlorides of Zr, Hf, Nb, Ta, Mo, W, Tc, Re, and Pt the metal ions are octahedrally coordinated by chloride ions, so that each metal ion shares four chloride ions with neighboring metal ions. The structures of these compounds differ primarily in the manner in which these chloride bridges are formed, and this is in turn apparently influenced by the degree of metal–metal interaction present. Chlorides of Zr,<sup>8</sup> Hf,<sup>8</sup> Tc,<sup>9</sup> and Pt<sup>10</sup> contain zigzag chains of MCl<sub>6</sub> octahedra sharing two edges such that the unshared chloride ions are cis; the metal–metal distances and magnetic moments for these compounds are consistent with the absence of metal–metal bonding. In NbCl<sub>4</sub>,<sup>11,12</sup> TaCl<sub>4</sub>,<sup>13</sup> α-MoCl<sub>4</sub>,<sup>14,15</sup> and WCl<sub>4</sub>,<sup>16</sup> the MCl<sub>6</sub> octahedra share opposite edges, and the metal–metal separations along the chains are alternately short and long, indicating a moderate degree of bonding between the paired metal ions. (β-MoCl<sub>4</sub>, the high-temperature polymorph, has the FeCl<sub>3</sub> structure and lacks metal–metal interactions.<sup>17</sup>) In ReCl<sub>4</sub>,<sup>18</sup> there are confacial bioctahedra which are then linked by shared chloride atoms, and within each bioctahedron the very short Re–Re distance, 2.728 (2) Å, indicates a bonding interaction.

It is easy to rationalize both the lack of bonding interactions between the d<sup>0</sup> metal ions in ZrCl<sub>4</sub> and HfCl<sub>4</sub> and the moderate metal–metal bonding present in d<sup>1</sup> NbCl<sub>4</sub> and TaCl<sub>4</sub> and d<sup>2</sup> α-MoCl<sub>4</sub> and WCl<sub>4</sub>. However, it is less clear why the metal–metal interactions in d<sup>3</sup> TcCl<sub>4</sub> and ReCl<sub>4</sub> should be so dissimilar. In order to better understand the trends in structure and metal–metal bonding in the transition metal tetrachlorides, we have determined the structure of the high-temperature form of OsCl<sub>4</sub> by single-crystal x-ray diffraction techniques.

An additional consideration underlying our interest in this compound was the fact that Os(IV) is a d<sup>4</sup> ion, isoelectronic with Cr(II), Mo(II), W(II), and Re(III), all of which form

compounds containing M–M quadruple bonds.<sup>19</sup> Thus, the question of whether the high charge in this case would overwhelm the tendency of a d<sup>4</sup> ion to engage in quadruple bond formation was clearly posed.

### Experimental Section

**Synthesis of OsCl<sub>4</sub>.** OsCl<sub>4</sub> was prepared by direct reaction of the elements using the method of Kolbin et al.<sup>3</sup> The procedure involves use of an L-shaped Pyrex reaction tube, where one leg of the tube contains Os powder and is heated to 525 °C while the other leg contains liquid chlorine at room temperature. The high pressure (6–8 atm) generated is necessary to prevent dissociation of the product to OsCl<sub>3</sub> and Cl<sub>2</sub>. The reaction was allowed to proceed for 5 days, by which time black crystals of OsCl<sub>4</sub> had formed in the hottest part of the tube. The crystals were not particularly air or water sensitive but were rather fragile, tending to crush into fine fibers when handled. A well-formed crystal of dimensions 0.139 × 0.083 × 0.300 mm was lightly coated with epoxy cement (to retard any slow reaction with the atmosphere) and was mounted for x-ray data collection.

**X-Ray Data Collection.** All data were collected at 21 ± 2 °C on a Syntex PI automated diffractometer using Mo Kα radiation monochromatized with a graphite crystal in the incident beam. The automatic centering and autoindexing procedures followed have been described elsewhere.<sup>20</sup> Preliminary photographs revealed orthorhombic symmetry. No systematic absences were evident other than those due to *C* centering ( $hkl$ ,  $h + k \neq 2n$ ), indicating *Cmmm*, *Cmm2*, and *C222* as possible space groups. The principal crystallographic data are as follows:  $a = 7.929$  (2),  $b = 8.326$  (2),  $c = 3.560$  (1) Å;  $V = 235.0$  (2) Å<sup>3</sup>,  $d_{\text{calcd}} = 4.69$  for  $Z = 2$  and a formula weight of 332.01.

A total of 221 unique reflections with  $0 < 2\theta \leq 50^\circ$  were collected using the  $\theta$ – $2\theta$  scan technique, variable scan rates from 4.0 to 24.0°/min, and a scan range from  $2\theta(\text{Mo K}\alpha_1) - 1.0^\circ$  to  $2\theta(\text{Mo K}\alpha_2) + 1.0^\circ$ . Intensities of three standard reflections measured after every 60 reflections showed no significant variation during data collection. Lorentz and polarization corrections and a numerical absorption correction<sup>21</sup> (linear absorption coefficient 308.83 cm<sup>-1</sup>) were applied. Transmission coefficients ranged from 0.0520 to 0.1512.

**Solution and Refinement of the Structure.** The structure was solved in the space group *Cmmm* (No. 65) and refined using all 221 unique reflections, all of which had  $F_o^2 > 3\sigma(F_o^2)$ . The positions of all atoms (Os, Cl(1), and Cl(2)) were determined using a three-dimensional Patterson function. The atomic coordinates and isotropic temperature factors were refined by three cycles of least-squares refinement to give the discrepancy indices (before application of the absorption correction)

$$R_1 = \sum |F_o| - |F_c| / \sum |F_o| = 0.248$$

$$R_2 = [\sum w(|F_o| - |F_c|)^2 / \sum w|F_o|^2]^{1/2} = 0.370$$